

# SCALABLE HIGH-ORDER ALGORITHMS FOR WAKEFIELD SIMULATIONS

Misun Min,\* Paul F. Fischer,

Mathematics and Computer Science, Argonne National Laboratory, Argonne, IL 60439, USA

## Abstract

We developed a high-order algorithm in time for our spectral-element discontinuous Galerkin time-domain electromagnetic code NekCEM. High-order spatial approximations are known to be the most efficient scheme guaranteeing a certain level of accuracy after long simulation time due to less numerical dispersion. We investigate an explicit type time stepping method, exponential time-integration method, based on Krylov approximation which can possibly accel efficiency by allowing larger time step size with the total number of timestep reduction for accelerator applications. Computational results are compared to those by the fourth-order Runge-Kutta method that has been widely used for high-order spatial operator for the Maxwell's equations. We demonstrate the parallel performance of the high-order time-integration scheme up to 8,192 processors achieving efficiency of 72%.

## INTRODUCTION

The electromagnetic solver NekCEM [1] is an Argonne-developed high-order Maxwell solver that employs a spectral-element discontinuous Galerkin (SEDG) scheme based on body-fitted hexahedral meshes [2, 3]. We have previously shown wakefield calculations using the fourth-order Runge-Kutta (RK4) time stepping method for the SEDG scheme [4, 5]. Here we discuss an efficient high-order time integration technique based on the Krylov subspace approximation [6] which allows larger timestep size as the dimension of the approximation space increases. We demonstrate some computational results of this method for accuracy and efficiency in comparison to the fourth-order Runge-Kutta method. Parallel performance on the high-order time integration method will be demonstrated.

## FORMULATIONS

This section describes the governing equations, discontinuous Galerkin formulation, and spectral discretizations in space.

### Maxwell's Equations

We consider the Maxwell's equations defined as

$$\mathbf{Q} \frac{\partial \mathbf{q}}{\partial t} + \nabla \cdot \mathbf{F}(\mathbf{q}) = \mathbf{S}, \quad (1)$$

where the field vector  $\mathbf{q}$  and the flux  $\mathbf{F}(\mathbf{q})$  are

$$\mathbf{q} = \begin{bmatrix} \mathbf{H} \\ \mathbf{E} \end{bmatrix}, \quad \mathbf{F}(\mathbf{q}) = \begin{bmatrix} F_H \\ F_E \end{bmatrix} = \begin{bmatrix} e_i \times \mathbf{E} \\ -e_i \times \mathbf{H} \end{bmatrix} \quad (2)$$

and the source term and material properties

$$\mathbf{S} = \begin{bmatrix} \mathbf{0} \\ -\mathbf{J} \end{bmatrix}, \quad \text{and} \quad \mathbf{Q} = \text{diag}(\mu, \mu, \mu, \epsilon, \epsilon, \epsilon), \quad (3)$$

where  $\mathbf{E} = (E_x, E_y, E_z)^T$ ,  $\mathbf{H} = (H_x, H_y, H_z)^T$ , and  $\mathbf{J}$  represent the electric, magnetic, and current fields, respectively, with the free space permittivity  $\epsilon$  and free space permeability  $\mu$ .

### The SEDG Approximations

We consider the computational domain  $\Omega$  with non-overlapping hexahedral elements  $\Omega^e$  such that  $\Omega = \cup_{e=1}^E \Omega^e$ . We have a weak formulation defined on each  $\Omega^e$  as in [4, 5]

$$\left( \mathbf{Q} \frac{\partial \mathbf{q}}{\partial t} + \nabla \cdot \mathbf{F}(\mathbf{q}) - \mathbf{S}, \phi \right)_{\Omega^e} = (\hat{n} \cdot [\mathbf{F} - \mathbf{F}^*], \phi)_{\partial \Omega^e} \quad (4)$$

where the numerical fluxes  $\mathbf{F}^*$  can be chosen as in [3].

We seek the local solutions of the fields in the form of  $q^N$  on each  $\Omega^e$  defined as

$$q^N(\mathbf{x}, t) = \sum_{i,j,k=1}^{N+1} q_{ijk} \psi_{ijk}(\mathbf{x}), \quad (5)$$

where  $q_{ijk}$  is the solution at  $\mathbf{x}=(x_i, y_j, z_k)$  on  $\Omega^e$ , and  $\psi_{ijk}=l_i(\xi)l_j(\eta)l_k(\gamma)$  where  $l_i$  is the one-dimensional Legendre Lagrange interpolation polynomial of degree  $N$  associated with the  $N + 1$  Gauss-Lobatto-Legendre quadrature nodes [2]. For simplicity, we describe the scheme with no source term in (4). We plug (5) into (4) with a local discontinuous test function  $\phi = \psi_{ijk}$  and apply the Gauss-Lobatto quadrature for the spatial integration and obtain a semi-discrete scheme as

$$\mu \mathbf{M} \frac{dH_x^N}{dt} = -(\mathbf{D}_y E_z^N - \mathbf{D}_z E_y^N) - \mathbf{R}(\mathbf{H}^N)_x, \quad (6)$$

$$\mu \mathbf{M} \frac{dH_y^N}{dt} = -(\mathbf{D}_z E_x^N - \mathbf{D}_x E_z^N) - \mathbf{R}(\mathbf{H}^N)_y, \quad (7)$$

$$\mu \mathbf{M} \frac{dH_z^N}{dt} = -(\mathbf{D}_x E_y^N - \mathbf{D}_y E_x^N) - \mathbf{R}(\mathbf{H}^N)_z, \quad (8)$$

$$\epsilon \mathbf{M} \frac{dE_x^N}{dt} = (\mathbf{D}_y H_z^N - \mathbf{D}_z H_y^N) - \mathbf{R}(\mathbf{E}^N)_x, \quad (9)$$

\* mmin@mcs.anl.gov

$$\epsilon \mathbf{M} \frac{dE_y^N}{dt} = (\mathbf{D}_z H_x^N - \mathbf{D}_x H_z^N) - \mathbf{R}(\mathbf{E}^N)_y, \quad (10)$$

$$\epsilon \mathbf{M} \frac{dE_z^N}{dt} = (\mathbf{D}_x H_y^N - \mathbf{D}_y H_x^N) - \mathbf{R}(\mathbf{E}^N)_z, \quad (11)$$

where the mass and stiffness matrices are defined as

$$\mathbf{M} = (\psi_{ijk}, \psi_{i\hat{j}\hat{k}})_{\Omega^e}, \mathbf{D}_x = \left( \frac{\partial \psi_{ijk}}{\partial x}, \psi_{i\hat{j}\hat{k}} \right)_{\Omega^e}, \quad (12)$$

$$\mathbf{D}_y = \left( \frac{\partial \psi_{ijk}}{\partial y}, \psi_{i\hat{j}\hat{k}} \right)_{\Omega^e}, \mathbf{D}_z = \left( \frac{\partial \psi_{ijk}}{\partial z}, \psi_{i\hat{j}\hat{k}} \right)_{\Omega^e} \quad (13)$$

and the surface integration as

$$\mathbf{R}(\mathbf{H}^N) = \left( \mathbf{n} \cdot [F_{\mathbf{H}} - F_{\mathbf{H}}^*], \phi_{i\hat{j}} \right)_{\partial \Omega^e}, \quad (14)$$

$$\mathbf{R}(\mathbf{E}^N) = \left( \mathbf{n} \cdot [F_{\mathbf{E}} - F_{\mathbf{E}}^*], \phi_{i\hat{j}} \right)_{\partial \Omega^e}. \quad (15)$$

## EXPONENTIAL TIME INTEGRATION

We study a Krylov-type high-order time integration method based on the Arnoldi algorithm for solving the Maxwell's equations. Recall the semi-discrete SEDG scheme defined in (6)-(11) that can be expressed by a system of ordinary differential equation as

$$q'(t) = \hat{A}q(t), \quad t > 0, \quad (16)$$

where  $q(t) = (q_1, q_2, \dots, q_n)^T$  is a vector and  $\hat{A}$  is a time-independent matrix of  $n \times n$ . The analytic solution of Eq. (16) can be written as

$$q(t) = e^{\hat{A}t} q(0). \quad (17)$$

Then the solution at  $(\bar{n} + 1)\Delta t$  can be expressed as

$$\underline{q}^{\bar{n}+1} = e^{\hat{A}\Delta t} \underline{q}^{\bar{n}}, \quad (18)$$

where  $\underline{q}^{\bar{n}} = q(\bar{n}\Delta t)$  for  $t = \bar{n}\Delta t$  and  $\bar{n} = 0, 1, 2, \dots$

We examine an explicit-type scheme for solving the linear systems approximately by using an iterative method. Letting  $A = \hat{A}\Delta t$  and  $\underline{q} = \underline{q}^{\bar{n}}$  for simplicity, the exponential term can be expanded in a Taylor series as, so that we have

$$e^A \underline{q} = \underline{q} + A\underline{q} + \frac{A^2}{2!} \underline{q} + \frac{A^3}{3!} \underline{q} + \dots \quad (19)$$

We consider the Krylov subspace of dimension  $m$ ,  $K_m(A, \underline{q})$ , approximating all possible polynomial approximations of degree at most  $m - 1$  including the truncated Taylor series,

$$K_m(A, \underline{q}) = \text{span}\{\underline{q}, A\underline{q}, A^2\underline{q}, \dots, A^{m-1}\underline{q}\}. \quad (20)$$

We seek a solution  $e^A \underline{q} \approx \underline{q}^{n+1} \in K_m(A, \underline{q})$ . The Arnoldi process [6] generates an orthonormal basis which can represent an element approximating  $e^A \underline{q}$ . The Arnoldi process is defined as follows.

## Arnoldi Process

1. Compute  $v_1 = \underline{q}/\|\underline{q}\|$ .
2. for  $j = 1, \dots, m$ 
  - (a)  $w = Av_j$ .
  - (b) Do  $i = 1, \dots, j$ 
    - i.  $h_{i,j} = (w, v_i)$
    - ii.  $w = w - h_{i,j}v_i$
  - (c) Compute  $h_{j+1,j} = \|w\|_2$  and  $v_{j+1} = w/h_{j+1,j}$  while  $h_{j+1,j} \neq 0$

The Arnoldi algorithm can be summarized as

$$V_{m+1}\bar{H} = AV_m, \quad (21)$$

where  $\bar{H} = [h_{i,j}] \in R^{(m+1) \times m}$  is an upper Hessenberg matrix. Defining  $H_m = [h_{i,j}] \in R^{m \times m}$  by deleting the  $(m + 1)$ -th row of  $\bar{H}$ , we can write Eq. (21) as

$$V_m H_m + h_{m+1,m} v_{m+1} e_m^T = AV_m, \quad (22)$$

where  $e_m$  is the  $m$ -th unit vector in  $R^m$ . We multiply  $V_m^T$  with (22) and then the second term in the left-hand side of Eq. (22) becomes a null matrix due to that  $V_m$  is an orthogonal matrix and we have  $V_m^T V_m = I$  for an  $m \times m$  identity matrix  $I$  since the Arnoldi vectors  $v_j$  are orthonormal, which leads to the following relation

$$H_m = V_m^T AV_m. \quad (23)$$

Thus we can write  $e^A \underline{q} \approx V_m e^{H_m} V_m^T \underline{q}$ . The large size of matrix exponential  $e^A$  of dimension  $n \times n$  is reduced to a lower-dimensional matrix exponential calculation  $e^{H_m}$  of dimension  $m \times m$  with the Krylov subspace projection.

For computing the matrix exponential  $e^{H_m}$ , we obtain eigenvalues of  $H_m$  using available library packages and compute ordinary exponential function with the eigenvalues.

## COMPUTATIONAL RESULTS

This section demonstrates the efficiency of the exponential time-integration algorithm with SEDG scheme including parallel performance.

### Convergence and CFL Increment

We present the study on the convergence of the SEDG exponential time integration method. In Figure 1, the top figure shows spatial convergence with a fixed  $m=11$  and timestep size. Depending on different resolution of the meshes, the errors decay exponentially as the spatial approximation order  $N$  increases. The bottom figure demonstrates the error behaviors depending on the approximation order in time  $m$  for a fixed resolution, provide with comparison to the RK4. The CFL number is increasing as  $m$  increases. We also observe that a higher order approximation in time allows a larger CFL number at a certain level of accuracy.

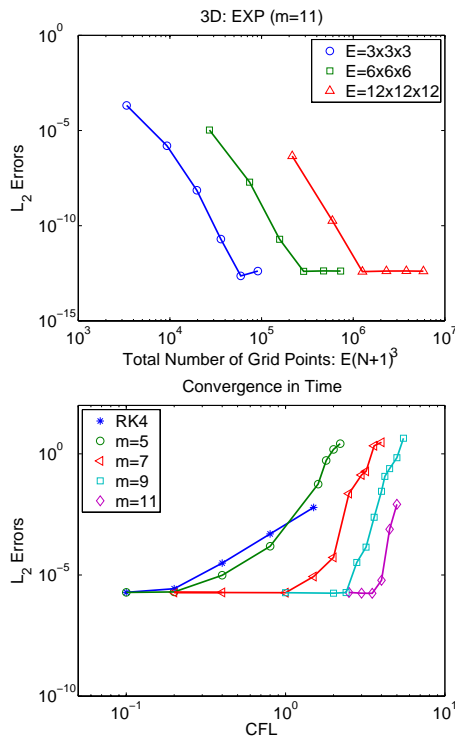


Figure 1: Spatial convergence (top) and temporal convergence (bottom) for  $m=5,7,9,11$ , in comparison to RK4 for the SEDG exponential time integration method.

Table 1: Parallel efficiency with  $E=22^3$ ,  $N=16$ , the total number of grid points  $\mathcal{N}=E(N+1)^3$  for a fixed order in time with  $m=7$  after 100 timesteps for the number of processors  $p=2,048, 4,096$ , and  $8,192$  with the number of grid points per processor  $\mathcal{N}/p$ .

Proc	$\mathcal{N}/p$	CPU(sec)	Ideal(sec)	Efficiency
2,048	25,543	7.085E+01	–	–
4,096	12,771	3.418E+01	3.542E+01	1.36
8,192	6,385	2.429E+01	1.771E+01	0.72

### Performance

We demonstrate the efficiency of the exponential time-integration algorithm with SEDG scheme. We consider the case with the temporal approximation order  $m=7$  for the number of elements  $E=22^3$  and the spatial approximation order  $N=16$  whose total number of grid points are  $\mathcal{N}=53,313,624$ . We perform strong-scaling test on Argonne Blue Gene/P for the number of processors  $p=2,048, 4096, 8192$ . Figure 2 shows the speedup depending on the processor counts. Table 1 shows the number of grid points per processor and efficiency.

### 05 Beam Dynamics and Electromagnetic Fields

### D06 Code Developments and Simulation Techniques

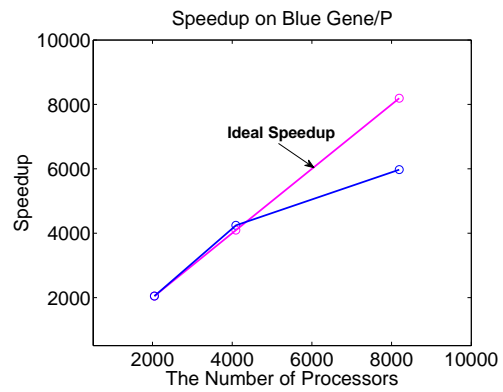


Figure 2: Parallel scalability for the SEDG exponential time integration scheme with  $m=7$  for the total number of grid points  $E(N+1)^3=53,313,624$  with  $E=22^3$ ,  $N=16$ .

## CONCLUSIONS

We have demonstrated an explicit-type high-order time-integration algorithm based on the Krylov subspace approximation for the semidiscrete form of the SEDG scheme. We show that one can take larger timestep size as the approximation order  $m$  increases so that computational cost can be reduced. We demonstrate some comparisons with RK4, provided with parallel efficiency for large-scale computing.

## ACKNOWLEDGMENT

This work was supported by the Office of Advanced Scientific Computing Research, Office of Science, U.S. Department of Energy, under Contract DE-AC02-06CH11357.

## REFERENCES

- [1] M.S. Min and P.F. Fischer, “NekCEM,” Mathematics and Computer Science Division, Argonne National Laboratory.
- [2] M.O. Deville, P.F. Fischer, and E.H. Mund, “High Order Methods for Incompressible Fluid Flow,” Cambridge University Press (2002).
- [3] J.S. Hesthaven and T. Warburton, “Nodal High Order Methods on Unstructured Grids - I. Time-Domain Solution of Maxwell’s Equations,” J. Comp. Physics, 101 (2002), p. 186. <https://svn.mcs.anl.gov/repos/NEKCEM>.
- [4] M.S. Min, P.F. Fischer, “Spectral-element discontinuous Galerkin simulations with a moving window algorithm for wakefield calculations”, Proc. of PAC09, TH5PFP03, 2009.
- [5] M.S. Min, P.F. Fischer, Y.C. Chae, “Wake fields for TESLA cavity structures: Spectral element discontinuous Galerkin simulations,” Proc. of SRF07, TUP34, 2007.
- [6] Y. Saad, Analysis of some Krylov subspace approximation to the matrix exponential operator, SIAM vol 29 (1992).